International Core Journal of Engineering Volume 10 Issue 5, 2024
ISSN: 2414-1895 DOI: 10.6919/ICJE.202405_10(5).0069

Laser Additive Manufactured Titanium Alloy: A Review on the Origin and Elimination of Anisotropy

Weiming Jia[1,*], Yuxin Shuai[1], Junbin Zhou[1], Xiaoying Guan[2], Xujie Tang[1], Min Chen[1], Weihui Liu[3]

[1] School of Material and Chemistry, University of Shanghai for Science and Technology, Yangpu, Shanghai 200093, China

[2] Jiangsu Vilory Advanced Materials Technology Co., Ltd, No. 2 Jingong Road, Gulou District, Xuzhou 221000, China

[3] College of Materials Science and Engineering, Inner Mongolia University of Technology, Hohhot, Inner Mongolia 010051, China

Abstract

Titanium alloys, as a lightweight metal material, have high specific strength and fracture toughness, and is a indispensable advanced engineering material in aerospace, energy and chemical industries. However, titanium alloys are difficult to process due to their poor thermal conductivity and low plastic deformation coefficient. Laser additive manufacturing (LAM) technology, as a new manufacturing method, could achieve the net-shape manufacturing of complex parts in a short time, providing a new way for the processing of titanium alloys. However, the directional deposition, rapid cooling rate and thermal cycle in LAM lead to the epitaxial growth of β columnar grains with solidification texture and martensitic transformation, resulting in low ductility and severe anisotropy of titanium alloy. In order to exert the design potential of LAM, especially for structural parts, it is necessary to optimize the microstructures and mechanical properties of titanium alloys through processing parameter and heat treatment optimization. This paper provides a comprehensive understanding of the anisotropy and mechanical property optimization of laser additive manufacturing titanium alloys. It mainly summarizes two LAM processes, laser powder bed fusion (LPBF) and direct laser deposition (DLD), and reviews the literature on the microstructure and mechanical property anisotropy of LAMed titanium alloys. Three methods for eliminating mechanical anisotropy, including element addition, process optimization, and post heat treatments, are highlighted. It can be emphasized that grain refinement and discontinuous GB-α are key factors in eliminating mechanical anisotropy. The advantages and disadvantages of existing methods are analyzed and compared, which can provide some reference for future research.

Keywords

Titanium Alloy; Laser Additive Manufacturing; Mechanical Property Anisotropy; Microstructure; Mechanical Properties.

1. Introduction

1.1 The Current Development Status of Titanium Alloys

Titanium alloy is a lightweight metal material with high specific strength and fracture toughness [1]. The application fields of titanium alloys are constantly expanding and have become one of the highly

ISSN: 2414-1895 DOI: 10.6919/ICJE.202405_10(5).0069

regarded materials in the field of engineering materials today [2]. In addition, titanium and titanium alloys, due to excellent mechanical properties and non-cytotoxicity, are often used as metallic bone implant materials and dental implant materials in the biomedical field [3,4]. In the meantime, titanium alloy has been widely used in ship anti fouling due to the excellent corrosion resistance [5]. Furthermore, the high stiffness and toughness of titanium alloys also make them commonly used in aerospace components such as aircraft landing gear, blade guides for rotorcraft, and helicopter rotor systems [6].

Titanium alloys can be classified into α-alloys, near-α alloys, α-β alloys, and β-alloys based on the strength and composition [1]. α-titanium alloys have excellent machinability and toughness, which are commonly used in aerospace fields. β titanium alloy is widely used in aerospace, chemical and energy industries because of its high specific strength, good toughness and excellent corrosion resistance, which can be effectively improved in the strength, ductility and fatigue properties by heat treatment [7]. α-β alloy is a titanium alloy that simultaneously contains α-phase and β-phase with higher strength and good formability.

1.2 Additive Manufacturing of Titanium Alloy

Due to the intrinsic physical and mechanical properties, such as poor thermal conductivity and low plastic deformation coefficient, titanium alloys are prone to adhesive and notch wear, as well as high temperature during cutting operations causes tool failure [8,9]. Therefore, conventional manufacturing methods face considerable challenges in producing titanium alloy components. The laser additive manufacturing (LAM) technology, as a novel manufacturing approach, enables the net-shape fabrication of intricate components within a short timeframe. It offers a new avenue for forming difficult-to-machine materials like titanium alloys [10].

Laser powder bed fusion (LPBF) and direct laser deposition (DLD) are two different additive technology processes [10–14]. LPBF is one of the most common additive manufacturing processes for producing metals/alloys with complex geometries and fine microstructures [10]. LPBF utilizes a laser beam to fuse metal powder particles layer-by-layer until the desired shape is achieved, based on computer-aided design (CAD) data. The LPBF was commonly used for rapid manufacturing in small batch production, which could fabricate parts with high density (> 99%) [15,16]. The schematic of the LPBF process is shown in Fig. 1 [17]. However, the LPBF may generate thermal stress and deformation during the manufacturing process. Thus, the process control of LPBF is very complex.

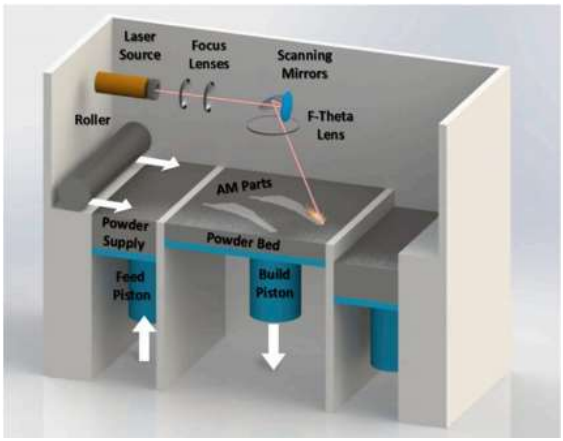

Fig. 1 Schematic of LPBF mechine. Reprinted from [17], Copyright 2018, with permission from Elsevier.

DLD technology is a commonly used additive manufacturing technique as well. It is based on a CAD model and utilizes a high-energy-density laser beam as a heat source to melt the material [18]. Additionally, DLD can deposit metal materials through powder or wire feeding, which provides high

ISSN: 2414-1895 DOI: 10.6919/ICJE.202405_10(5).0069

manufacturing efficiency and flexibility. In comparison to other laser additive manufacturing technologies, DLD enables functional material grading, rapid repair and cladding, as well as multi-axis deposition. Simultaneously, it offers high material utilization, short production cycles, and lower costs as compared to traditional manufacturing methods [19].

In general, LPBF and DLD both involve melting metal powder layer-by-layer with lasers to fabricate parts. They are also capable of creating complex geometries and customized parts as well, which offer high design freedom. However, DLD has a faster manufacturing rate, while LPBF exhibits higher manufacturing flexibility. LPBF has a higher degree of manufacturing precision and surface quality to some extent, and is capable of producing smaller-sized structures. On the contrary, DLD has a relatively larger manufacturing size range [20].

1.3 The Mechanical Property Anisotropy of LAMed Titanium Alloys

LAMed titanium and titanium alloys are widely concerned due to their high strength, corrosion resistance, and high-temperature resistance. However, their inherent anisotropy makes them prone to the formation of defects, plastic deformation, and residual stress, thereby affecting the performance of processed parts. This presents significant challenges for the application of titanium and titanium alloys in various fields. The anisotropy of mechanical properties of additive manufactured titanium alloy is caused by the combination of temperature gradient of molten pool, grain orientation during solidification, thermal stress and residual stress. Therefore, it is important to eliminate the anisotropy of titanium and titanium alloys. In this paper, we will systematically introduce and summarize the methods for eliminating the anisotropy of LAMed titanium alloys.

2. The Microstructure in the LAMed Titanium Alloys

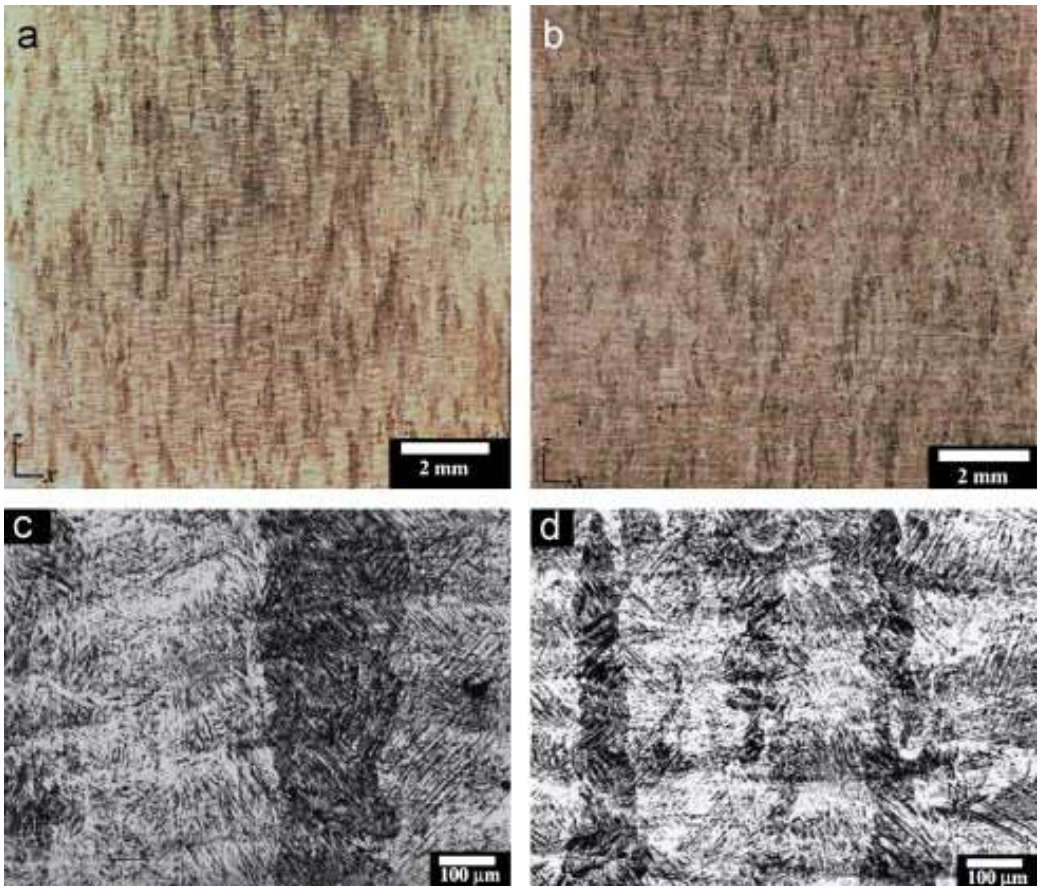

Fig. 2 The optical micrographs (OM) depict a predominant columnar grain structure in (a, c)vertically fabricated samples and (a, c) horizontally fabricated samples for fabricated Ti-6Al-4V by LPBF. Reprinted from [23], Copyright 2013, with permission from Elsevier.

ISSN: 2414-1895 DOI: 10.6919/ICJE.202405_10(5).0069

During the process of additive manufacturing, metal powders are melted by a high-energy beam, which causes localized temperature to increase instantly to the melting point and then forms a molten pool in a short period. It also forms a high-temperature gradient between the previous deposition layers. The grains grow in a direction perpendicular to the molten pool boundary, manifested as columnar grains growing through the melt pool or along the building direction (Fig. 2) [21–23].

Different manufacturing processes of additive manufacturing result in different microstructures of titanium alloys. For instance, it is reported that the Ti-6Al-4V has a non-equilibrium microstructure caused by directional solidification, rapid cooling rate and thermal cycling during the LPBF process. Thus, the columnar prior-β grains grow epitaxially in the opposite heat transfer direction, with strong <100> solidification texture [24–31]. In addition, due to the extremely high cooling rate of LPBF and the diffusion-less transformation dominates, the fine acicular α′ martensite precipitate in the prior-β grains, which has a weak $\{11\bar{2}0\}$ texture [32,33]. The α′ martensite has very high strength and low ductility. Moreover, the residual stresses are induced in the LPBF process owing to the high-temperature gradient [16].

The microstructure of DLD Ti-6Al-4V consists mainly of columnar prior-β grains growing in the faster cooling direction (Fig. 3a) [34]. Meanwhile, the rapid cooling after the solidification could cause many fine Widmanstätten α to precipitate at the grain boundaries (Fig. 3b) [35,36]. Likewise, the microstructure reported in DLD Ti-6.5Al-2Zr-1Mo-1V alloy consists of coarse columnar grains, which grow along the building direction [34,37].

Similarly, large <001> oriented columnar prior-β grains were formed along the building direction in the α titanium alloy TA15 (Ti-6Al-2Zr-1Mo-1V) fabricated by LPBF (Fig. 4) [38]. However, the GB-α (grain boundary α) phase is observed along the prior-β grain after the heat treatments. The GB-α phase follows the Burgers orientation relationship (BOR) with the matrix prior-β grains [39,40]. The presence of continuous GB-α could facilitate crack propagation along grain boundaries, which significantly hinders the enhancement of mechanical properties. The DLD TA15 alloy consists of an acicular α″+α martensitic phase, which could transform into the Widmanstätten structure after heat treatments (such as the anneal treatment with water or air cooling) [41].

The electron back scatter Diffraction (EBSD) results (Fig. 5) show the presence of the α/α′ phase in Ti-15Mo alloys fabricated by LPBF, which is attributed to the trapped oxygen in the interstitial space between powders [42]. Oxygen is an effective α stabilizer and titanium alloys containing 0.4 wt% oxygen increase the β-transition temperature by 50 K, which promotes the precipitation of the α/α′ phase [43]. Furthermore, the intensity of the α′ phase is weak compared to the strong peaks of the β-phase in Ti-15Mo alloys [42].

It is worth mentioning that, as a research hotspot in recent years, the structural design of lattice structures has also attracted widespread attention for the study of mechanical anisotropy. Lightweight lattice structures have broad application prospects in biomedical scaffolds, energy absorption, structural components, and other fields [44,45]. In addition, lattice structures often have predictable failure mechanisms and high damage tolerance[46]. AM has solved the challenge of structural complexity at microscopic dimensions for lattice structures due to its high precision and near-net shape. Therefore, it is possible to solve the macroscopic mechanical anisotropy of lattice structures through structural design. The design of horizontally distributed struts can improve the spatial anisotropy of lattice structures and reduce the possibility of shear failure [47]. However, it should be noted that for isotropic loaded lattice structures (such as diamond unit cell), poor-quality horizontal struts can lead to early failure of the structure [48]. At the same time, a unique topology optimized (TO) unit cell was proposed [49]. TO lattice exhibits high yield strength and plateau stress levels. When loaded in different directions, this structure exhibits nearly isotropic energy absorption and low mechanical anisotropy.

ISSN: 2414-1895 DOI: 10.6919/ICJE.202405_10(5).0069

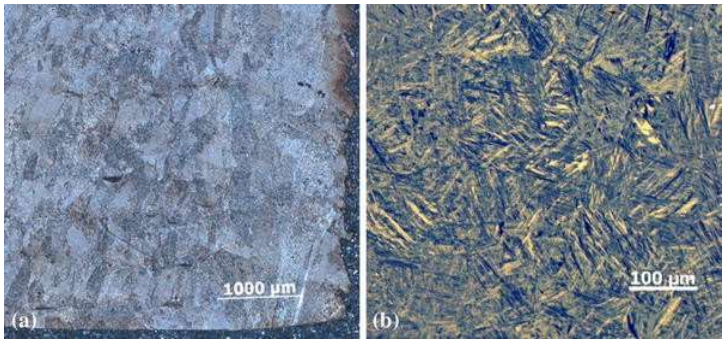

Fig. 3 In the fabricated Ti-6Al-4V by DLD, (a) the macrostructure consists of fine columnar grains, and (b) the microstructure exhibits a very fine Widmanstätten structure. Reprinted from [34], Copyright 2015, with permission from Springer Nature.

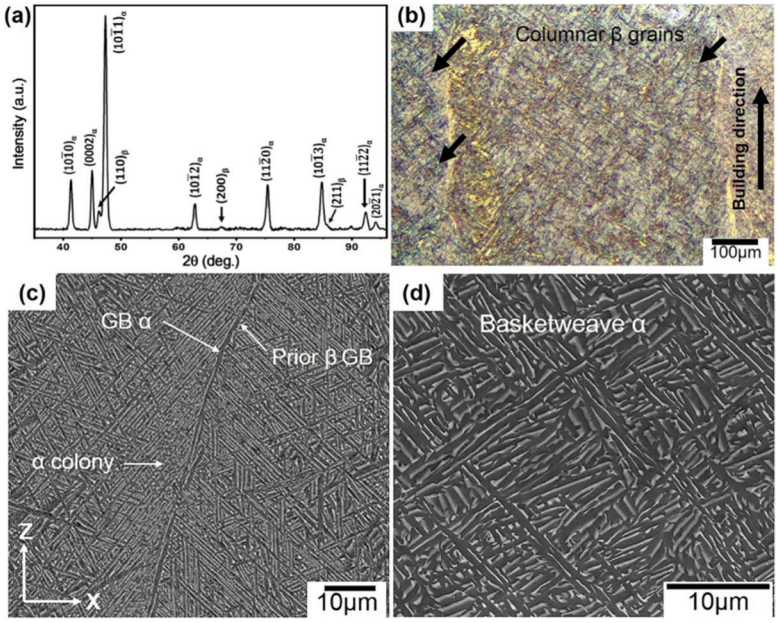

Fig.4 Manufacturing characteristics of LPBF TA15 alloy: (a) XRD pattern; (b) OM image depicting columnar β grains; (c) SEM surface view displaying parallel α-colonies along the prior β grain boundary (GB); and (d) magnified image revealing basket-like α structure. Reprinted from [38] , Copyright 2021 with permission from Springer Nature.

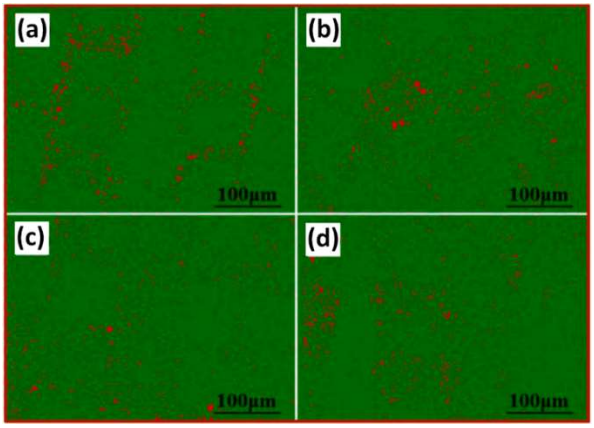

Fig.5 Identifying the phase of four scanning strategies through EBSD, the angle of each over-building layer is shifted by (a) 0°, (b) 45 °, (c) 90°,and (d) chessboard (red areas indicate α/α′ phases and green areas indicate β-phases). Reprinted from [42], Copyright 2015, with permission from Elsevier.

ISSN: 2414-1895 DOI: 10.6919/ICJE.202405_10(5).0069

3. Mechanical Property Anisotropy Elimination by Element Additions

The generation of columnar β grains in additive-manufactured titanium alloys is due to the steep temperature gradient from the melt pool to the substrate and the narrow solidification range [10,26,50–52]. Columnar grains are one of the main reasons causing anisotropy in LAMed titanium alloys [53–55]. Several recent studies have shown that the addition of specific alloying elements (La, Cu, and B) or very small amounts of nanoparticles can play an important role in generating additional nucleation sites in the molten pool and transforming the columnar grains into an equiaxed grains [56–61].

Adding β stable elements Cr and Mo in titanium alloys could enhance the compositional supercooling, which made the single β-phase microstructure refined and equiaxed [62]. During the process of fabricating Ti-6Al-4V by DLD, Co-28Cr-6Mo (CCM) powder was mixed with Ti-6Al-4V powder in a ritio of 12:1 and 40:7. Respectively, expressed as 5Co and 10Co based on Co content. And the compositional supercooling and β-phase stability of the specimens were enhanced after adding the two powders in a Ti-6Al-4V: CCM ratio of 40:7. Due to the higher solubility of Co in β-alloy (~ 17.3 wt.%) compared to its solubility in α-alloy (~ 1 wt.%), the formation of intermetallic compounds can be prevented by stabilizing the β-phase [63]. It resulted in a refined equiaxed single β-phase structure (grain size of approximately 36 μm) with a random texture and isotropic tensile characteristics [64]. In Fig. 6, the 10Co samples with a Ti-6Al-4V to CCM ratio of 40:7 exhibit a strong combination of properties, including a yield strength of 941 ± 25 MPa and a tensile elongation of 14.2 ± 2.1%. Due to the 10Co sample, in the repeated heating cycles during the DLD process, a completely stable β microstructure was obtained without any α precipitation at the grain boundary (GB). The special microstructure can avoid the brittle fracture and achieve the isotropic tensile properties[64].

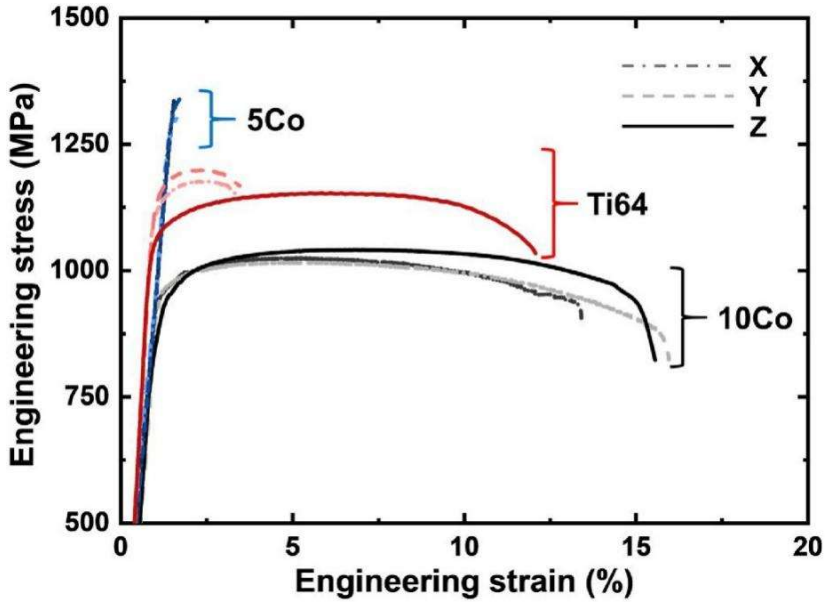

Fig. 6 Engineering stress-strain curves of Ti-6Al-4V, 5Co, and 10Co. Reprinted form [64], Copyright 2020, with permission from Elsevier.

Recent research has indicated that during the LAM process, adding a small amounts of metallic rare earth elements (REEs) to the alloy composition can effectively refine grains and improve the mechanical properties of the alloys. For example, during the LAM process, the introduction of La elements into the β matrix forms a La-rich liquid (Ll) that affects the microstructural evolution of titanium alloys. Through the Ll + β → α transition, α particles nucleate in the Ll + β field and then transition from β (β → α) [64,65]. The resulting α-phase is not always oriented in the same direction as the parent β-phase, thus greatly reducing texture and achieving an equiaxed microstructure[66,67]. Fig. 7 (a) shows a portion of the Ti-2wt% La binary phase diagram [56]. Fig. 7 (b-g) shows that the

ISSN: 2414-1895 DOI: 10.6919/ICJE.202405_10(5).0069

addition of La transforms the typical needle-shaped α′ martensitic structure in titanium alloys into partially equiaxed α grains. This transformation is due to the L1 +β→La-bcc peritectoc reaction that takes place in the LPBF process. In addition, a comparison of pole figure confirms the reduction of texture in the microstructure after the addition of La elements.

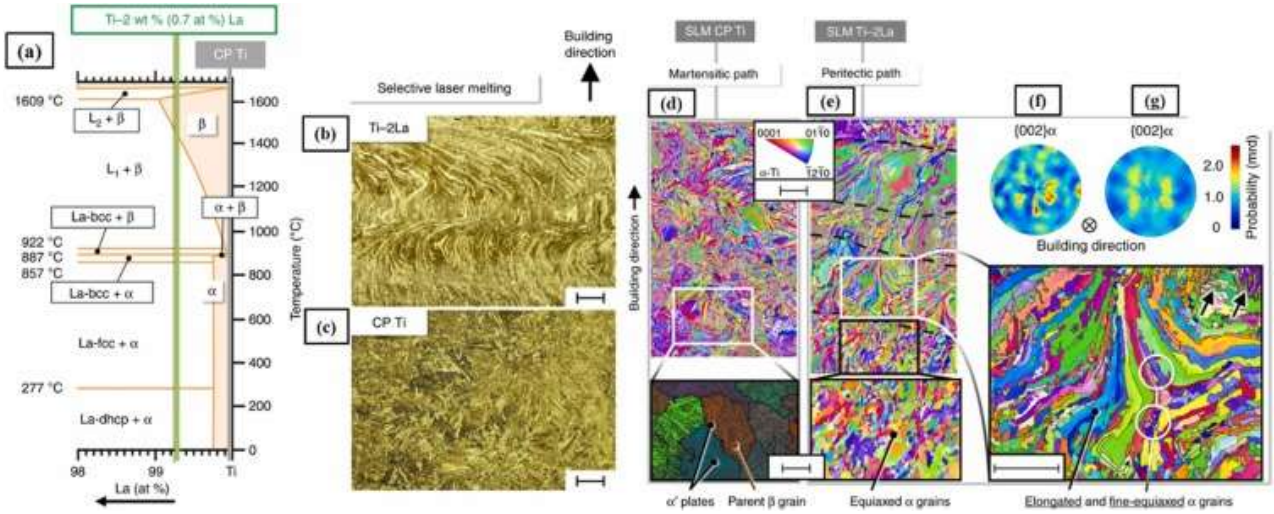

Fig. 7 (a) Fragment of Ti-La binary equilibrium phase diagram for Ti-2 wt% La; (b, c) OM image of microstructure of LPBF Ti-2 wt% La alloy and CP-Ti. The scale in the image is 100μm. EBSD images and polar coordinates of (d, f) LPBF CP-Ti and (e, g) LPBF Ti-2 wt%La alloy. The scale and magnification area of EBSD images are 100μm and 50μm, respectively. Reprinted from [56], Copyright 2018, with permission from Springer Nature.

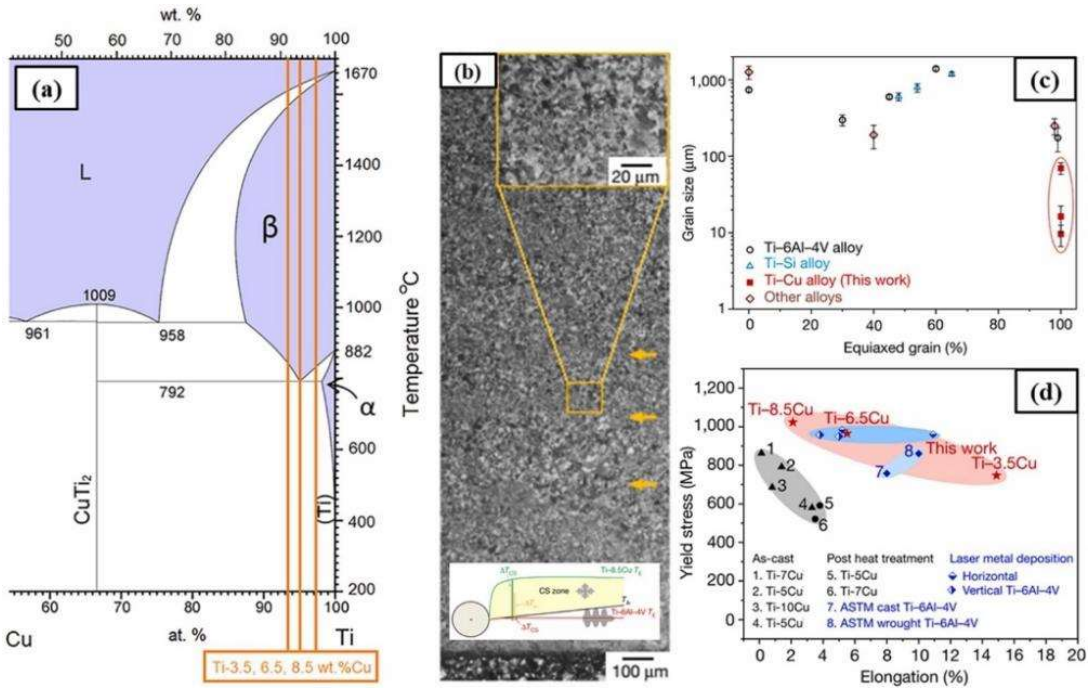

Fig. 8 (a) On the titanium-rich side of the Ti-Cu binary phase diagram, the components of Ti-3.5, 6.5, and 8.5 wt% Cu are classified as low eutectic, eutectic, and hypereutectic, respectively. (b) Optical microscope (OM) images of DLD Ti-8.5wt% Cu at low and high magnification. (c) The area percentage and grain size of equiaxed grainsand (d) Yield stress and elongation of Ti-3.5, 6.5 and 8.5wt% Cu alloys and other Ti alloys manufactured by different methods. Reprinted from [57] , Copyright 2019, with permission from Springer Nature.

ISSN: 2414-1895 DOI: 10.6919/ICJE.202405_10(5).0069

In the DLD process, adding Cu (as an available low-cost element) to pure titanium can also eliminate the anisotropy of LAMed parts. Fig. 8a depicts the Ti-rich side of the Ti-Cu binary phase diagram, showing that adding 3.5, 6.5, and 8.5 wt% of Cu to Ti leads to Cu partitioning during the LAM process. This occurs due to a large supercooling capacity, which changes the microstructure from columnar to equiaxed [57]. In Fig. 8b, an SEM image of Ti-8.5 wt% Cu reveals an equiaxed microstructure with ultrafine grains. Fig. 8c shows the correlation between grain size and the percentage of equiaxed grains in different titanium alloys produced by different fabrication methods. As shown in Fig. 8d, the addition of copper to titanium alloys increases the proportion of equiaxed grains with smaller grain sizes, which synergistically increases strength and conductivity. It is clear that in the titanium binary alloy system, the addition of copper not only refines the β-phase titanium grain, but also promotes the formation of eutectic microstructures. The extremely fine eutectic microstructure improves the strength and ductility of the LAMed specimens [68].

Recent studies have explored adding non-metallic elements/nucleating agents like ceramic B4C and Y2O3 to titanium alloys treated with AM [69,70]. The effect of the addition of trace amounts of B4C (0.2 wt%) under as-fabricated and heat-treated conditions on the microstructure and the mechanical properties of LPBF Ti-6Al-4V have been studied. Adding B4C particles in Ti-6Al-4V could dissolve B and create TiB precipitated phases. The needle-like TiB organization restricts primitive β grain growth. It could also prevent the nucleation and growth of the α-phase from the β → α phase transition. After heat treatment at 1050°C, the microstructure is fully equiaxed prior-β grains and the tensile strength is enhanced to 1400 MPa with 40% elongation, eliminating the effect of the harmful GB-α phase.

4. Mechanical Property Anisotropy Elimination by LAM Process Optimization

The titanium alloy formed by additive manufacturing exhibits significant anisotropy due to the formation of β columnar grains, especially DLD titanium alloy, is likely to fail to meet the minimum mechanical performance requirements of the Aerospace Materials Specification (AMS) standards [71]. In order to eliminate the anisotropy in titanium alloys formed by additive manufacturing, in addition to element addition, researchers also attempted process optimization to transform the original columnar grains into equiaxed grains with weaker textures.

The laser processing mode has a direct impact on the microstructure of the fabricated titanium alloy. Research has found that in the continuous wave (CW) laser processing mode, the microstructure of Ti-6Al-4V is large columnar grains, while the pulse wave (PW) laser mode tends to form fine equiaxed grains (Fig. 9) [66]. This is attributed to the instability of the molten pool under PW mode based on thermal flow, which suppresses the growth of grains across the molten pool [67]. However, the potential to adjusting laser parameters is very limited. In addition, higher laser power will form a coarser microstructure, which is not conducive to the improvement of mechanical properties of titanium alloy. In LPBF Ti-6Al-4V lattice structure, the PW mode makes the microstructure more homogenous and finer, while also exhibiting mechanical isotropy [72]. The strut thickness of PW specimens are more uniform, so compared to CW, this scanning mode can be recommended for smaller components that require dimensional accuracy, such as lattice structures. However, it should be pointed out that due to high porosity and a large number of partially melted particles, the process parameters of PW need further optimization.

The commonly used methods for microstructure control of formed titanium alloys are thermomechanical processes (such as rolling). In this method, room-temperature or low-temperature rollings are usually used to achieve better grain refinement. However, the rolling process requires significant stress, which greatly reduces the lifespan of the machine.

ISSN: 2414-1895 DOI: 10.6919/ICJE.202405_10(5).0069

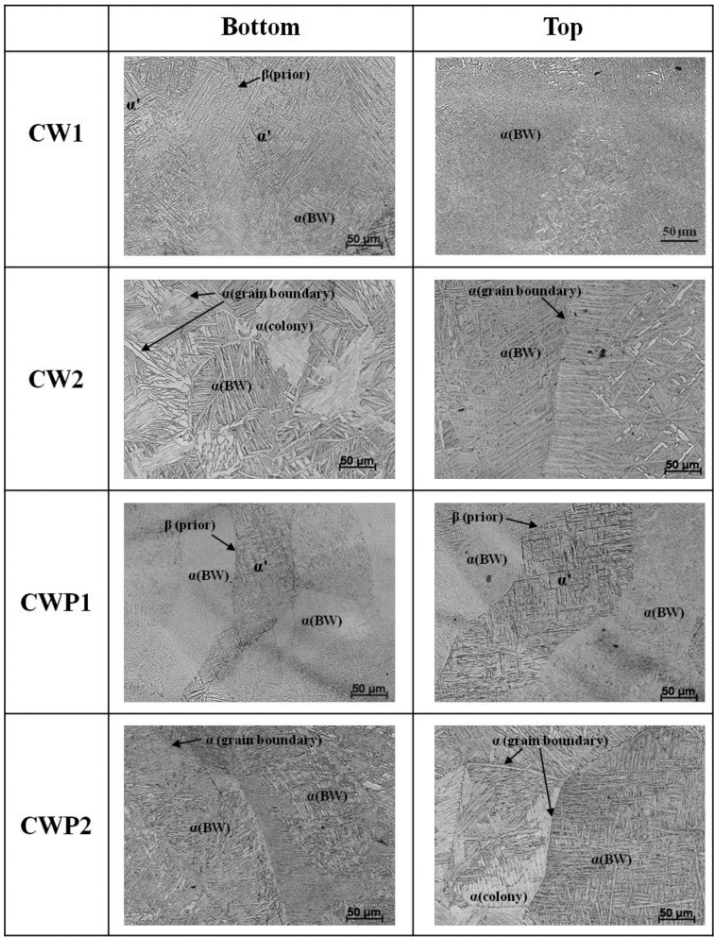

Fig. 9 OM images of the top (left) and bottom (right) microstructures of DLD Ti-6Al-4V under different laser modes and paramenters (CWP refers to CW+PW mode). Reprinted from [73], Copyright 2016, with permission from Elsevier.

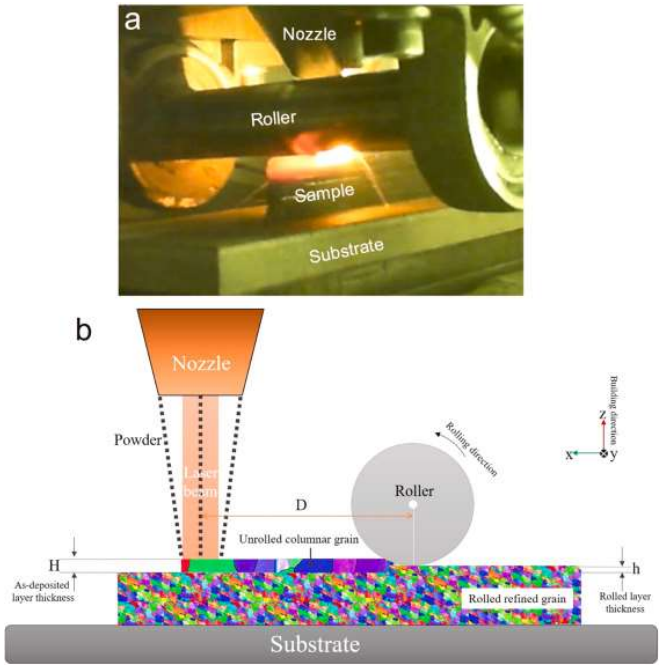

Fig. 10 (a) The actual DLD in-situ rolling image, and (b) DLD in-situ rolling demonstration diagram. Reprinted from [71], Copyright 2021, with permission from Elsevier.

ISSN: 2414-1895 DOI: 10.6919/ICJE.202405_10(5).0069

To solve this problem, research has designed a high-temperature in-situ rolling process to achieve simultaneous forming and heat treatment, thereby refining the microstructure of titanium alloys (Fig. 10a) [71]. As show in Fig. 10b, the principle of this technology is to accurately control the deformation by selecting the appropriate rolling process parameters, for instance rolling temperature, rolling speed and reduction levels [74,75]. The goal is to optimize the microstructure, eliminate anisotropy in the material's mechanical properties, and achieve more uniform mechanical properties. This uniform performance can enhance the reliability and stability of engineering applications and improve the material mechanical properties, particularly ductility and fatigue resistance.

The yield strength (YS) and ultimate tensile strength (UTS) in the Ti-6Al-4V sample increased by about 20% along the building direction after in-situ rolling, and in the test sample perpendicular to the building direction, the YS and UTS increased by about 12% (Fig.) [71]. More importantly, the mechanical properties of DLD Ti-6Al-4V in the horizontal and building directions are extremely close. The improvement of mechanical properties and elimination of anisotropy are mainly due to grain refinement (Fig.).

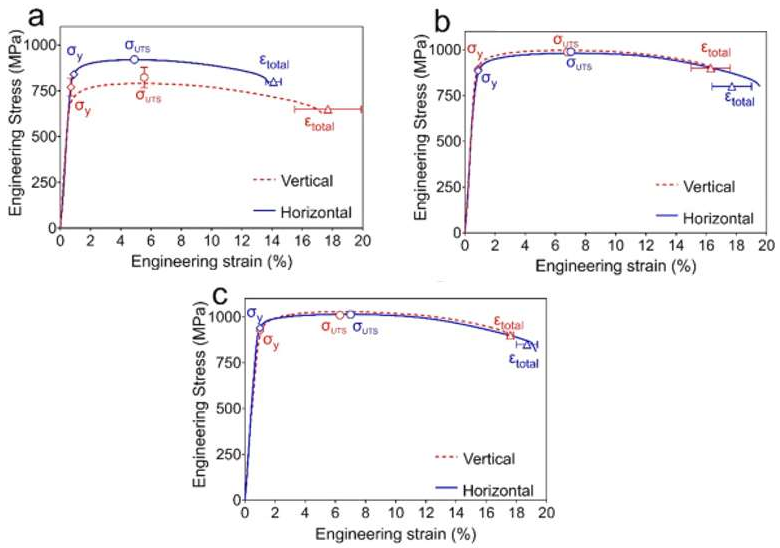

Fig. 11 Stress-strain curves of Ti-6Al-4V formed by different forming processes: (a) DLD Ti-6Al-4V; In situ rolling DLD Ti-6Al-4V under (b) 37.5% and (c) 50% nominal reduction. Reprinted from [71], Copyright 2016, with permission from Elsevier.

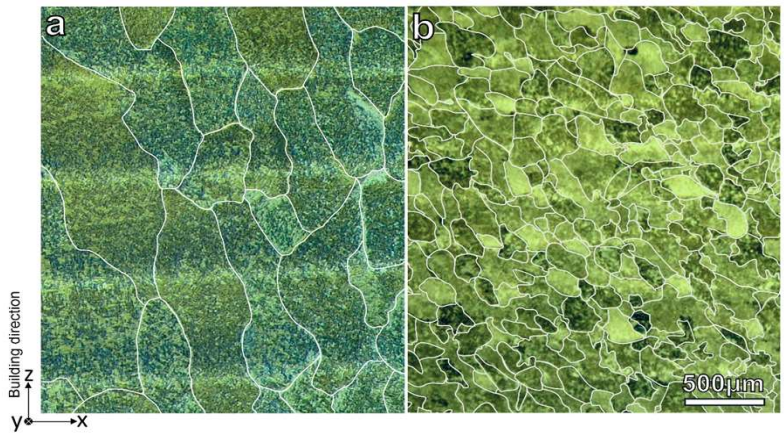

Fig. 12 OM images of Ti-6Al-4V formed by different forming processes: (a) DLD Ti-6Al-4V, (b) in situ rolling DLD Ti-6Al-4V. Reprinted from [71], Copyright 2021, with permission from Elsevier.

ISSN: 2414-1895 DOI: 10.6919/ICJE.202405_10(5).0069

Similar to the principle of changing the PW laser mode, using high-intensity ultrasound to stir the solution can also achieve grain refinement. High-intensity ultrasound activates the nucleation centers in the alloy, thereby suppressing the formation of columnar grains and forming new fine grains. In order to achieve a fine microstructure, it is necessary to optimize process parameters, including offset, loading angle, and ultrasonic input amplitude. [76]. It is reported that a study introduces ultrasonic vibration technology, using high-intensity ultrasound to synchronously load and influence the laser and wire additive manufacturing (LWAM) Ti-6Al-4V alloy layer [77]. The incorporation of high-intensity ultrasound effectively disrupts the epitaxial growth pattern of the dendrites, refining the microstructure of the titanium alloy to a certain extent, and producing a large number of equiaxed grains in the final deposition layer. Moreover, the simultaneous ultrasonic energy-assisted method is versatile and can accommodate complex component shapes.

This high-intensity ultrasonic treatment for enhancing microstructures applies to various alloy systems produced via LAM. As show in Fig. 13, employing high-intensity ultrasound in DLD Ti-6Al-4V led to the columnar-to-equiaxed transition and improved the mechanical properties [76]. Ultrasonic cavitation proves effective in suppressing the formation of columnar grains and improving the microstructure of metallic materials [78]. This green, environmentally friendly, and pollution-free method has opened up a new research direction for incorporating materials in the manufacturing of titanium alloys, showing potential for practical engineering applications.

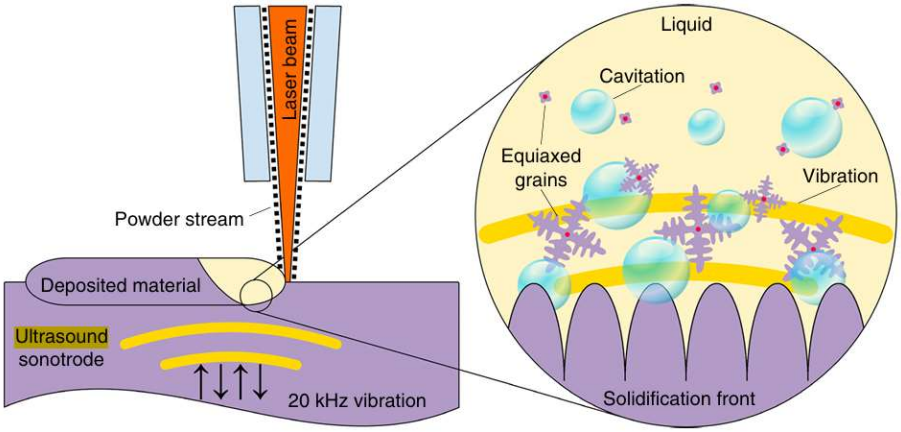

Fig. 13 The demonstration diagram of the forming process of DLD Ti-6Al-4V based on ultrasonic assistance and local magnification demonstrates the working principle of ultrasonic waves. Reprinted from [76], Copyright 2020, with permission from Springer Nature.

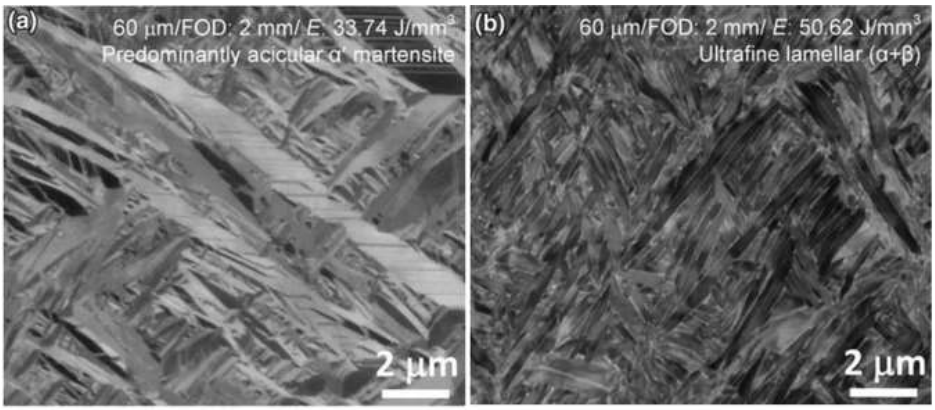

Fig. 14 SEM images of microstructure under different thermal and magnetic field environments: energy density of (a) 30.74 J/mm3 and (b) 50.62 J/mm3. Reprinted from [79], Copyright 2015, with permission from Springer Nature.

ISSN: 2414-1895 DOI: 10.6919/ICJE.202405_10(5).0069

Current research suggests that the application of a magnetic field has the potential to alter the thermodynamic state of material phase transitions and affect the process of phase transformation. This indicates a significant relationship between magnetic fields and phase transitions. Therefore, the application of magnetic fields provides a method to improve the microstructure and mechanical properties of LPBF Ti-6Al-4V alloy. As show in Fig. 14, this coupling effect promotes the phase transition from α′→α+β, and the width of α'/α phases can be changed [79].

5. Mechanical Property Anisotropy Elimination by Post-heat Treatment

As mentioned above, one of the main reasons for the significant anisotropy in the mechanical properties of LAMed titanium alloys is the prior-β columnar grains [79–82]. Post-heat treatment is a commonly used method for regulating the microstructural morphology in titanium alloys[83–85]. Some reports also indicate that after post-heat treatment, columnar grains transform into equiaxed grains, significantly weakening the texture, and the microstructure and mechanical properties achieve isotropy [86]. At the same time, under water quenching conditions, the continuity of GB-α in LAMed Ti–6Al–4V decreases, further eliminating the anisotropy of the microstructure [87].

Fig. 15 shows the microstructure of the XOY (vertical to buiding direction) and XOZ (parallel to building direction) surfaces of the Ti–6Al–4V[88]. As can be seen from Fig. 15b,d, the α-phase microstructure of heat-treated Ti–6A l–4V is basket-like, while α laths are coarsening. During annealing, the prior-β GB is destroyed, and the β columnar grains transforms into equiaxed ones. Therefore, there is no significant anisotropy in the microstructure.

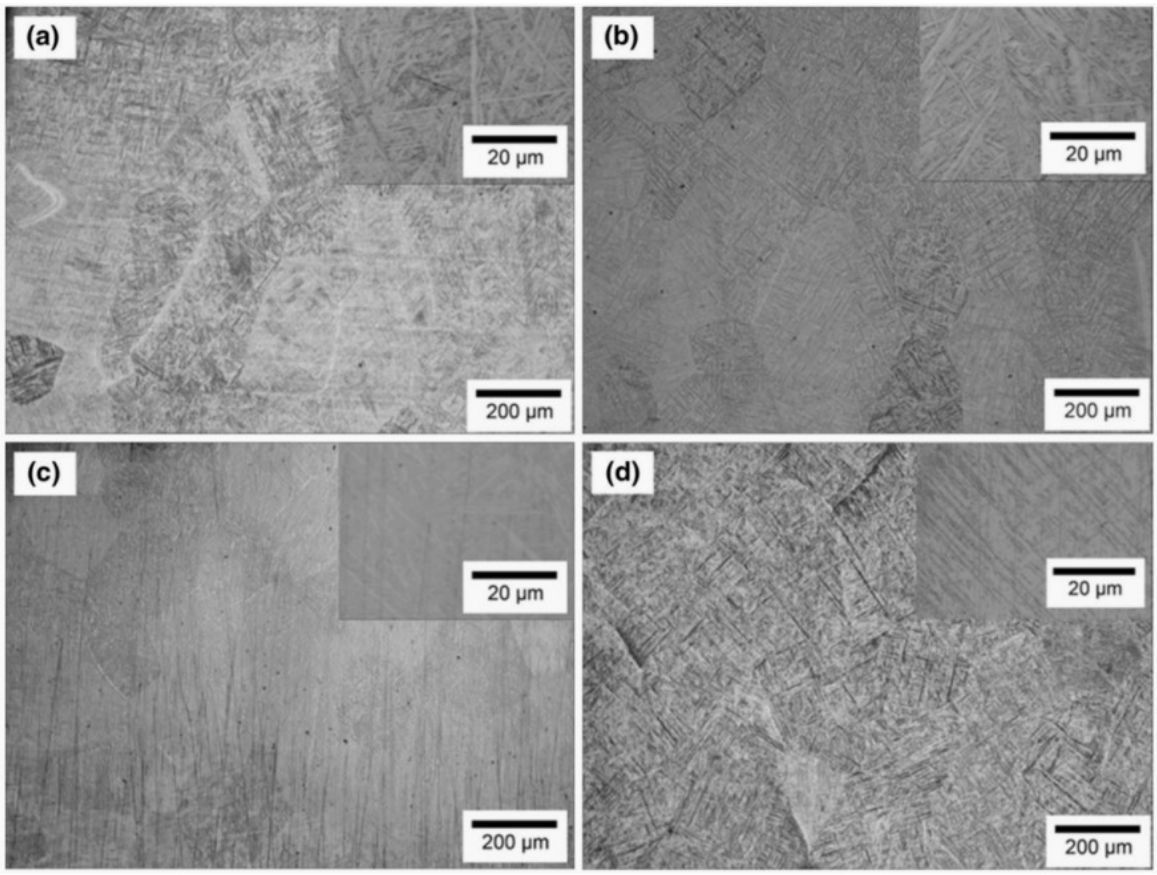

Fig. 15 Microstructure of annealed titanium samples: (a, b) small substrate; (c, d) large substrate. Reprinted from [88], Copyright 2015, with permission from Springer Nature.

Fig. 16 shows the hardness of XOY, YOZ, and XOZ cross sections [89]. It can be found that the Vickers hardness (HV) of the XOY cross-section of the as-fabricated LPBF Ti-6Al-5V is higher than

ISSN: 2414-1895 DOI: 10.6919/ICJE.202405_10(5).0069

the YOZ and XOZ cross-section There are a large number of fine equiaxed crystals distributed in the XOY section, and a large number of grain boundaries provide sufficient resistance to dislocation slip deformation. After annealing, the hardness of all sections increased, and the hardness of the XOY section was similar to that of the YOZ and XOZ sections, which were both about 400 HV. It is because a large number of fine secondary α-phases precipitated during the annealing process and attached to the primary α lath or GBα phases, which caused the α lath and GB-α phases to constantly coarsening, and dislocation density increases. Then, the coarsening α laths leads to a more inhomogeneous distribution between β-phases, and the resistance to the dislocation slip motion between each other increases, resulting in an overall increasing in the hardness. The microstructure of all cross-sections shows the basket-like microstructure, with the discontinuous distribution of GB-α and relatively strong coordinated deformation of the coarsening α-phase, resulting in similar hardness and weakened anisotropy in all sections.

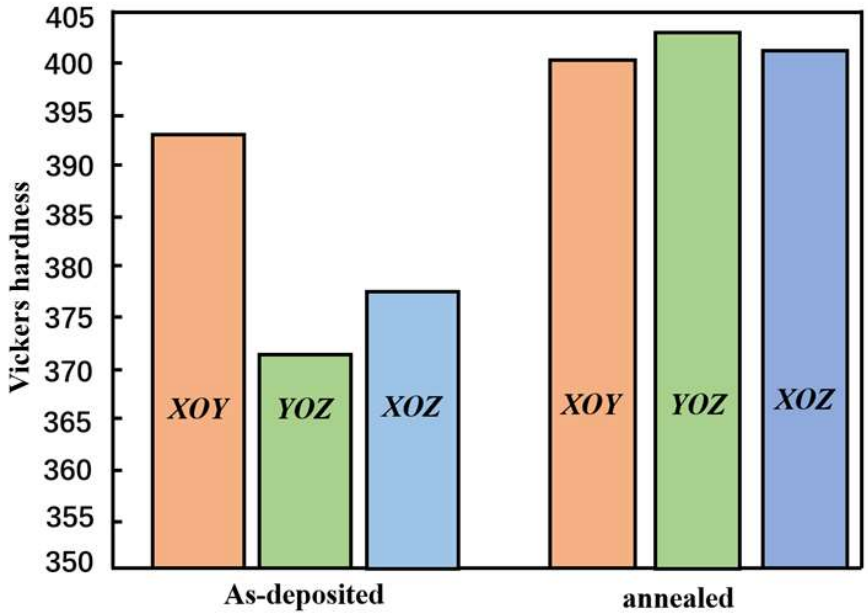

Fig. 16 Hardness of different cross-sections of Ti-6Al-4V samples.

However, the research has also pointed out that even if the prior β columnar grains transform into equiaxed grains, there still exists anisotropy in the tensile properties and texture [90]. Typical α+β titanium alloy Ti–6.5Al–3.5Mo–1.5Zr–0.3Si (TC11) samples were fabricated using the DLD method, and subjected to α+β-HT (1000°C/ 1h + 530°C/6h) and β-HT (1030°C/ 1h) heat treatments. The microstructural characterization results show that the as-fabricated sample has obvious molten pool and columnar grains, and the grains of the sample after β-HT transformation are transformed into equiaxed grains (Fig.17b-d, f). After α + β-HT, DLD TC11 still exhibits columnar grains growing across the molten pool (Fig.17e). Further XRD and EBSD characterization results show that although β-HT TC11 exhibits equiaxed grains, its microstructure still exhibits strong β<001>direction texture (Fig. 18d). This is attributed to the presence of prior columnar microstructures within equiaxed grains, leading to the formation of strong textures. And these strong textures cannot be eliminated by β-HT, resulting in the anisotropy of mechanical properties as shown in Table 1. Therefore, it is extremely important to conduct research on the post-heat treatment process for different LAM titanium alloys. More in-depth research is also needed on the mechanism of eliminating mechanical anisotropy through post-heat treatment.

ISSN: 2414-1895 DOI: 10.6919/ICJE.202405_10(5).0069

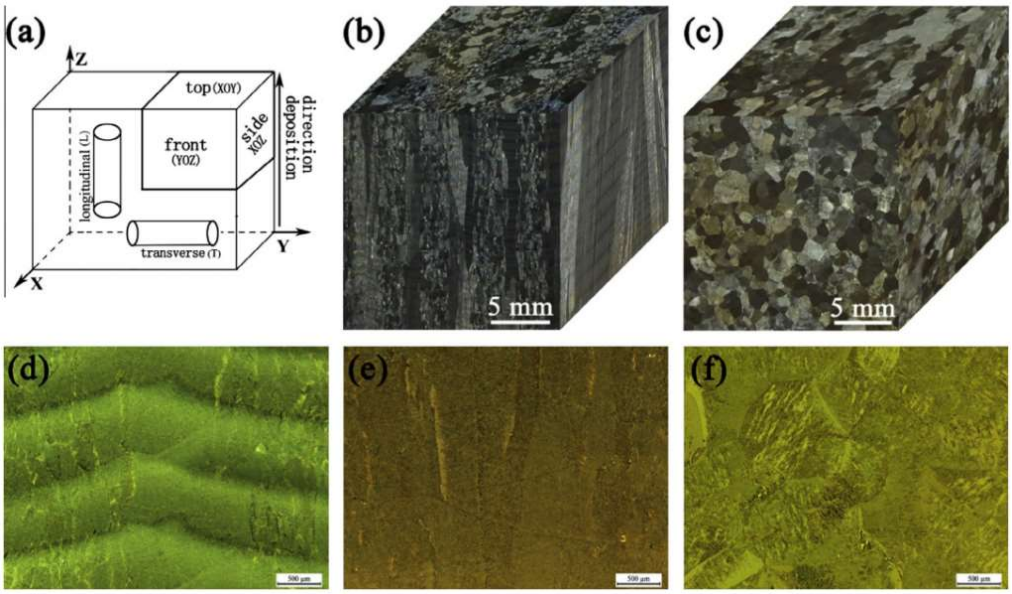

Fig. 17 (a) Stretch sample model; Optical mirror (OM) image representation: (b) as build LAM TC11 3D image, (c) HT LAM TC11 3D image; Microstructure of (d) as build LAM TC11, (e) α + β-HT LAM TC11, and (f) β-HT LAM TC11 at high magnification. Reprinted from [90], Copyright 2015, with permission from Elsevier.

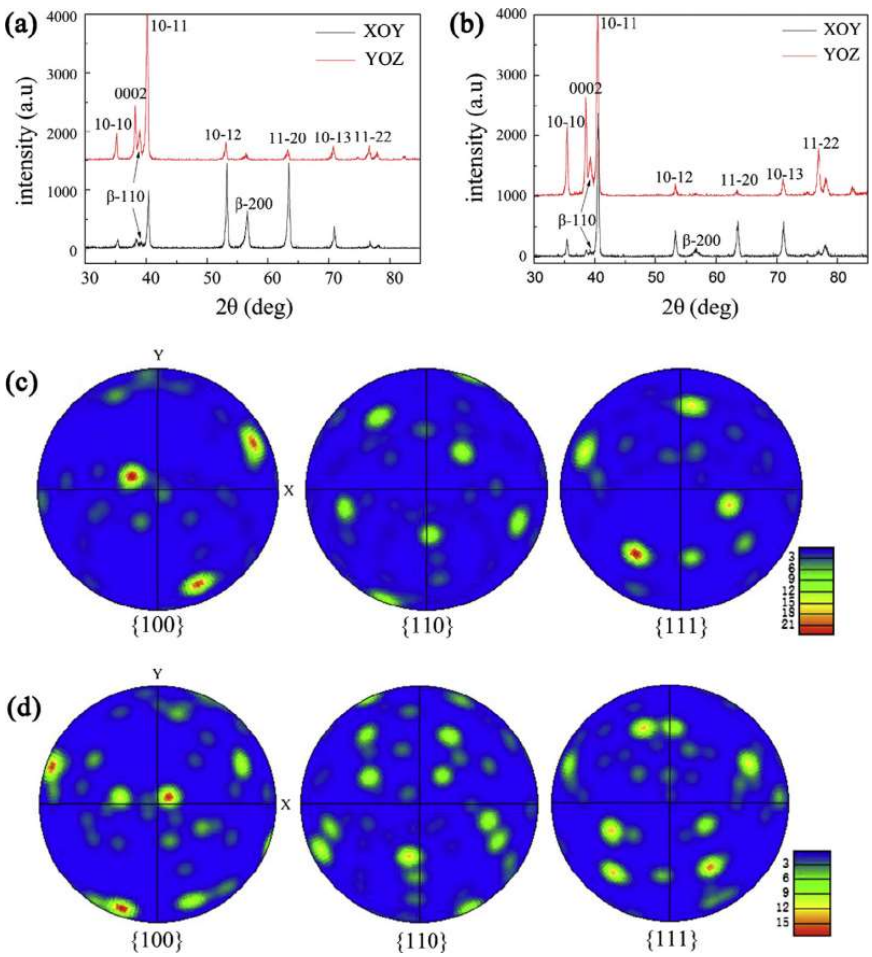

Fig. 18 XRD results of (a) α + β-HT TC11 and (b) β-HT TC11; EBSD results of (c) α + β-HT TC11 and (d) β-HT TC11. Reprinted from [90], Copyright 2015, with permission from Elsevier.

ISSN: 2414-1895 DOI: 10.6919/ICJE.202405_10(5).0069

Table 1. Room temperature tensile test results. Reprinted from [90], Copyright 2015, with permission from Elsevier.

Samples	Directions	UTS (MPa)	YS (MPa)	EL (%)	RA (%)
As-fabricated	Vertical	1018.00	932.00	14.70	28.40
	Horizontal	1089.00	1001.00	9.90	15.80
α + β-HT	Vertical	1033.00	895.00	16.80	40.00
	Horizontal	1099.0	971.00	11.80	22.30
β-HT	Vertical	1038.0	895.0	10.00	16.30
	Horizontal	1059.0	915.0	9.00	13.70
Specification	-	≥950.0		≥6.00	≥14.00

6. Summary

1) Titanium alloy is widely used in the aerospace, biomedical, shipbuilding and automotive fields because of its light weight, corrosion resistance and outstanding strength-to-weight ratio. Additive manufacturing processes, such as LPBF and DLD, have emerged as innovative approaches aimed at overcoming barriers to efficient production of titanium components. The anisotropy of titanium alloys is affected by the grain orientation, which challenges the uniformity of its properties. The anisotropy of LPBF and DLD processes in additive manufacturing is characterized by the formation of columnar and dendrite grains due to local temperature increase and excessive cooling rate. The anisotropy of mechanical properties of additive manufactured titanium alloy is caused by the combination of temperature gradient of molten pool, grain orientation during solidification, thermal stress and residual stress. LPBF produces non-equilibrium delamination and articulated α 'martensite, while DLD exhibits fine wiedemannstaten and basket-like. Therefore, understanding and mitigating this anisotropy is critical to optimizing the potential of titanium alloys in a variety of applications.

2) Recent studies have shown that the addition of specific alloying elements or nanoparticles can transform columnar structures into equiaxial structures, eliminating anisotropy. Adding Cr, Mo, La, Cu, B and other elements can refine the structure and improve the mechanical properties. For example, the addition of Cu results in a higher proportion of equiaxed grains with small grain sizes, resulting in a better strength-plasticity synergy. In addition, the addition of a small amount of B4C can form a completely isotropic structure with high ultimate tensile strength and elongation

3) The current effective mechanical methods could improve the microstructure of DLD titanium alloys include pulsed wave (PW) laser scanning, in situ rolling, high-intensity ultrasound and magnetic field action. The influence mechanism of PW and high intensity ultrasound is similar, both of which control the growth of columnar grains by controlling the molten pool and providing new grain shaped nuclear energy.

4) Directional solidification in the LPBF process leads to the formation of β columnar grains. However, the microstructure of the alloy is transformed into equiaxed grains after heat treatment, the braided microstructure is obviously weakened, and the microstructure and mechanical properties of the alloy achieve isotropy. Citation isometric β and discontinuous GB-α which lead to an increase in dislocation density within the alloy and resistance to dislocation slip. The closer hardness makes the anisotropy weaker.

Author Contributions

Conceptualization, W.J.; methodology, W.J.; validation, J.Z., L.W., and X.G.; formal analysis, M.C., and T.X.; resources, Q.C.; writing-original draft preparation, W.J. and M.C.; writing-review and

ISSN: 2414-1895 DOI: 10.6919/ICJE.202405_10(5).0069

editing, J.Z and Y.S.; visualization, W.J., and T.X.; supervision, X.G. and Q.C.; funding acquisition, Y.S. All authors have read and agreed to the published version of the manuscript.

Data Avaliability Statement

The data presented in this study are available on request from the corresponding author.

References

[1] P. Pushp, S.M. Dasharath, C. Arati, Classification and applications of titanium and its alloys, Mater. Today Proc. 54 (2022) 537–542. https://doi.org/10.1016/j.matpr.2022.01.008.

[2] D. Liu, C. Ni, Y. Wang, L. Zhu, Review of serrated chip characteristics and formation mechanism from conventional to additively manufactured titanium alloys, J. Alloys Compd. 970 (2024) 172573. https://doi.org/10.1016/j.jallcom.2023.172573.

[3] X. Han, J. Ma, A. Tian, Y. Wang, Y. Li, B. Dong, X. Tong, X. Ma, Surface modification techniques of titanium and titanium alloys for biomedical orthopaedics applications: A review, Colloids Surfaces B Biointerfaces. 227 (2023) 113339. https://doi.org/10.1016/j.colsurfb.2023.113339.

[4] X. Chen, A. Kolooshani, B. Heidarshenas, B. Mortezagholi, Y. Yuan, D.T. Semiruomi, Effects of tricalcium phosphate-titanium nanoparticles on mechanical performance after friction stir processing on titanium alloys for dental applications, Mater. Sci. Eng. B. 293 (2023) 116492. https://doi.org/10.1016/j.mseb.2023.116492.

[5] U. Nichul, V. Hiwarkar, Carbon dot complimentary green corrosion inhibitor for crystallographically textured Beta C titanium alloy for marine application: A state of art, J. Alloys Compd. 962 (2023) 171116. https://doi.org/10.1016/j.jallcom.2023.171116.

[6] D.B. Anant Sagar, Y. Pardhu, M.S.K. Rao, N. Narasaiah, Strain hardening behavior of friction welded beta titanium alloy Titan 1023 used for aeronautical applications, Mater. Today Proc. 57 (2022) 687–692. https://doi.org/10.1016/j.matpr.2022.02.113.

[7] S.S.S. Kumar, B. Pavithra, V. Singh, P. Ghosal, T. Raghu, Tensile anisotropy associated microstructural and microtextural evolution in a metastable beta titanium alloy, Mater. Sci. Eng. A. 747 (2019) 1–16. https://doi.org/10.1016/j.msea.2019.01.053.

[8] W. Dong, H. Gao, C. Guo, T. Dong, Z. Yang, H. Li, F. Jiang, Effect of additive manufacturing process and heat treatment on microstructure and properties of Ti-6Al-4V alloy, Hangkong Cailiao Xuebao/Journal Aeronaut. Mater. 42 (2022) 22–32. https://doi.org/10.11868/j.issn.1005-5053.2022.000064.

[9] E.O. Ezugwu, Z.M. Wang, Titanium alloys and their machinability - A review, J. Mater. Process. Technol. 68 (1997) 262–274. https://doi.org/10.1016/S0924-0136(96)00030-1.

[10] T. DebRoy, H.L. Wei, J.S. Zuback, T. Mukherjee, J.W. Elmer, J.O. Milewski, A.M. Beese, A. Wilson-Heid, A. De, W. Zhang, Additive manufacturing of metallic components – Process, structure and properties, Prog. Mater. Sci. 92 (2018) 112–224. https://doi.org/10.1016/j.pmatsci.2017.10.001.

[11] S. Liu, Y.C. Shin, Additive manufacturing of Ti6Al4V alloy: A review, Mater. Des. 164 (2019) 107552. https://doi.org/10.1016/j.matdes.2018.107552.

[12] J. Fan, L. Zhang, S. Wei, Z. Zhang, S.K. Choi, B. Song, Y. Shi, A review of additive manufacturing of metamaterials and developing trends, Mater. Today. 50 (2021) 303–328. https://doi.org/10.1016/j.mattod.2021.04.019.

[13] A. Ambrosi, R.R.S. Shi, R.D. Webster, 3D-printing for electrolytic processes and electrochemical flow systems, J. Mater. Chem. A. 8 (2020) 21902–21929. https://doi.org/10.1039/d0ta07939a.

[14] C. Sun, Y. Wang, M.D. McMurtrey, N.D. Jerred, F. Liou, J. Li, Additive manufacturing for energy: A review, Appl. Energy. 282 (2021). https://doi.org/10.1016/j.apenergy.2020.116041.

[15] T. Tinga, Effects of powder reuse on the microstructure and mechanical behaviour of Al – Mg – Sc – Zr alloy processed by laser powder bed fusion (LPBF), 36 (2020). https://doi.org/10.1016/j.addma. 2020.101625.

[16] F.I. Jamhari, F.M. Foudzi, M.A. Buhairi, A.B. Sulong, N.A. Mohd Radzuan, N. Muhamad, I.F. Mohamed, N.H. Jamadon, K.S. Tan, Influence of heat treatment parameters on microstructure and mechanical

ISSN: 2414-1895 DOI: 10.6919/ICJE.202405_10(5).0069

performance of titanium alloy in LPBF: A brief review, J. Mater. Res. Technol. 24 (2023) 4091–4110. https://doi.org/10.1016/j.jmrt.2023.04.090.

[17] H. Shipley, D. McDonnell, M. Culleton, R. Coull, R. Lupoi, G. O'Donnell, D. Trimble, Optimisation of process parameters to address fundamental challenges during selective laser melting of Ti-6Al-4V: A review, Int. J. Mach. Tools Manuf. 128 (2018) 1–20. https://doi.org/10.1016/j.ijmachtools.2018.01.003.

[18] C. Lv, J. Wang, H. Li, Q. Yin, W. Liu, S. Shen, Dynamics of the laser–powder interaction in the Ti6Al4V powder feeding process of laser-directed energy deposition additive manufacturing, J. Mater. Res. Technol. 27 (2023) 6376–6385. https://doi.org/10.1016/j.jmrt.2023.11.099.

[19] G. Ma, T. Di, C. Song, F. Niu, J. Lu, D. Wu, Phase transformation mechanism and mechanical properties of Ti-45Al-8Nb alloy prepared by directed laser deposition, Mater. Charact. 193 (2022) 112256. https://doi.org/10.1016/j.matchar.2022.112256.

[20] D. Ochs, K.K. Wehnert, J. Hartmann, A. Schiffler, J. Schmitt, Sustainable Aspects of a Metal Printing Process Chain with Laser Powder Bed Fusion (LPBF), Procedia CIRP. 98 (2021) 613–618. https://doi.org/10.1016/j.procir.2021.01.163.

[21] Q. Guo, C. Zhao, M. Qu, L. Xiong, L.I. Escano, S.M.H. Hojjatzadeh, N.D. Parab, K. Fezzaa, W. Everhart, T. Sun, L. Chen, In-situ characterization and quantification of melt pool variation under constant input energy density in laser powder bed fusion additive manufacturing process, Addit. Manuf. 28 (2019) 600–609. https://doi.org/10.1016/j.addma.2019.04.021.

[22] W.E. King, A.T. Anderson, R.M. Ferencz, N.E. Hodge, C. Kamath, S.A. Khairallah, A.M. Rubenchik, Laser powder bed fusion additive manufacturing of metals; physics, computational, and materials challenges, Appl. Phys. Rev. 2 (2015) 041304. https://doi.org/10.1063/1.4937809.

[23] C. Qiu, N.J.E. Adkins, M.M. Attallah, Microstructure and tensile properties of selectively laser-melted and of HIPed laser-melted Ti-6Al-4V, Mater. Sci. Eng. A. 578 (2013) 230–239. https://doi.org/10.1016/j.msea.2013.04.099.

[24] L.E. Murr, S.A. Quinones, S.M. Gaytan, M.I. Lopez, A. Rodela, E.Y. Martinez, D.H. Hernandez, E. Martinez, F. Medina, R.B. Wicker, Microstructure and mechanical behavior of Ti-6Al-4V produced by rapid-layer manufacturing, for biomedical applications, J. Mech. Behav. Biomed. Mater. 2 (2009) 20–32. https://doi.org/10.1016/j.jmbbm.2008.05.004.

[25] E. Sallica-Leva, R. Caram, A.L. Jardini, J.B. Fogagnolo, Ductility improvement due to martensite α' decomposition in porous Ti-6Al-4V parts produced by selective laser melting for orthopedic implants, J. Mech. Behav. Biomed. Mater. 54 (2016) 149–158. https://doi.org/10.1016/j.jmbbm.2015.09.020.

[26] W. Xu, M. Brandt, S. Sun, J. Elambasseril, Q. Liu, K. Latham, K. Xia, M. Qian, Additive manufacturing of strong and ductile Ti-6Al-4V by selective laser melting via in situ martensite decomposition, Acta Mater. 85 (2015) 74–84. https://doi.org/10.1016/j.actamat.2014.11.028.

[27] M. Simonelli, Y.Y. Tse, C. Tuck, Effect of the build orientation on the mechanical properties and fracture modes of SLM Ti-6Al-4V, Mater. Sci. Eng. A. 616 (2014) 1–11. https://doi.org/10.1016/j.msea. 2014.07.086.

[28] M. Simonelli, Y.Y. Tse, C. Tuck, On the texture formation of selective laser melted Ti-6Al-4V, Metall. Mater. Trans. A Phys. Metall. Mater. Sci. 45 (2014) 2863–2872. https://doi.org/10.1007/s11661-014-2218-0.

[29] L. Thijs, F. Verhaeghe, T. Craeghs, J. Van Humbeeck, J.P. Kruth, A study of the microstructural evolution during selective laser melting of Ti-6Al-4V, Acta Mater. 58 (2010) 3303–3312. https://doi.org/10.1016/j.actamat.2010.02.004.

[30] S. Cao, Z. Chen, C.V.S. Lim, K. Yang, Q. Jia, T. Jarvis, D. Tomus, X. Wu, Defect, Microstructure, and Mechanical Property of Ti-6Al-4V Alloy Fabricated by High-Power Selective Laser Melting, Jom. 69 (2017) 2684–2692. https://doi.org/10.1007/s11837-017-2581-6.

[31] T. Vilaro, C. Colin, J.D. Bartout, As-fabricated and heat-treated microstructures of the Ti-6Al-4V alloy processed by selective laser melting, Metall. Mater. Trans. A Phys. Metall. Mater. Sci. 42 (2011) 3190–3199. https://doi.org/10.1007/s11661-011-0731-y.

[32] T. Ahmed, H.J. Rack, Phase transformations during cooling in alpha + beta titanium alloys, Mater. Sci. Eng. A. 243 (1998) 206–211.

ISSN: 2414-1895 DOI: 10.6919/ICJE.202405_10(5).0069

[33] A. Pathania, A.K. Subramaniyan, B.K. Nagesha, Influence of post-heat treatments on microstructural and mechanical properties of LPBF-processed Ti6Al4V alloy, Prog. Addit. Manuf. 7 (2022) 1323–1343. https://doi.org/10.1007/s40964-022-00306-6.

[34] L. Bian, S.M. Thompson, N. Shamsaei, Mechanical Properties and Microstructural Features of Direct Laser-Deposited Ti-6Al-4V, Jom. 67 (2015) 629–638. https://doi.org/10.1007/s11837-015-1308-9.

[35] M. Hedges, N. Calder, Near net shape rapid manufacture & repair by LENS, Cost Eff. Manuf. via Net-Shape Process. Meet. Proc. RTO-MP-AVT-139, Pap., 2006.

[36] J. Alcisto, A. Enriquez, H. Garcia, S. Hinkson, T. Steelman, E. Silverman, P. Valdovino, H. Gigerenzer, J. Foyos, J. Ogren, J. Dorey, K. Karg, T. McDonald, O.S. Es-Said, Tensile properties and microstructures of laser-formed Ti-6Al-4V, J. Mater. Eng. Perform. 20 (2011) 203–212. https://doi.org/10.1007/s11665-010-9670-9.

[37] X. HE, T. WANG, X. WANG, W. ZHAN, Y. LI, Fatigue behavior of direct laser deposited Ti-6.5Al-2Zr-1Mo-1V titanium alloy and its life distribution model, Chinese J. Aeronaut. 31 (2018) 2124–2135. https://doi.org/10.1016/j.cja.2018.09.003.

[38] M. Rizwan, J. Lu, F. Chen, R. Chai, R. Ullah, Y. Zhang, Z. Zhang, Microstructure Evolution and Mechanical Behavior of Laser Melting Deposited TA15 Alloy at 500 ° C under In - Situ Tension in SEM, Acta Metall. Sin. (English Lett. 34 (2021) 1201–1212. https://doi.org/10.1007/s40195-021-01214-4.

[39] J. Lu, L. Sang, Y. Xiaoxiao, W. Zhang, Y. Zhang, Z. Zhang, In-situ tensile deformation behavior of as-built laser direct metal deposited Ti-6Al-4V alloy at 200℃, 817 (2020) 1–9. https://doi.org/10.1016/j.jallcom.2019.152781.

[40] E. Lee, R. Banerjee, S. Kar, D. Bhattacharyya, H.L. Fraser, Selection of α variants during microstructural evolution in α/β titanium alloys, Philos. Mag. 87 (2007) 3615–3627. https://doi.org/10.1080/ 1478643 0701373672.

[41] S.A. Shalnova, O.G. Klimova-Korsmik, A. V. Arkhipov, F.A. Yunusov, Structure and properties of near-α titanium products obtained by direct laser deposition and heat treatment, J. Phys. Conf. Ser. 2077 (2021). https://doi.org/10.1088/1742-6596/2077/1/012018.

[42] L. Zhou, J. Sun, X. Bi, J. Chen, W. Chen, Y. Ren, Y. Niu, C. Li, W. Qiu, T. Yuan, Effect of scanning strategies on the microstructure and mechanical properties of Ti–15Mo alloy fabricated by selective laser melting, Vacuum. 205 (2022) 111454. https://doi.org/10.1016/j.vacuum.2022.111454.

[43] H. Xu, Z. Li, A. Dong, H. Xing, T. Zhang, D. Wang, G. Zhu, B. Sun, Study of superior strength in Ti15Mo alloy manufactured using selective laser melting, J. Alloys Compd. 885 (2021) 161186. https://doi.org/10.1016/j.jallcom.2021.161186.

[44] M.G. Rashed, M. Ashraf, R.A.W. Mines, P.J. Hazell, Metallic microlattice materials: A current state of the art on manufacturing, mechanical properties and applications, Mater. Des. 95 (2016) 518–533. https://doi.org/10.1016/j.matdes.2016.01.146.

[45] D.J. Yoo, Porous scaffold design using the distance field and triply periodic minimal surface models, Biomaterials. 32 (2011) 7741–7754. https://doi.org/10.1016/j.biomaterials.2011.07.019.

[46] L.R. Zeng, L.Y. Wang, P.T. Hua, Z.P. He, G.P. Zhang, In-situ investigation of dwell fatigue damage mechanism of pure Ti using digital image correlation technique, Mater. Charact. 181 (2021). https://doi.org/10.1016/j.matchar.2021.111466.

[47] X. Yan, Q. Li, S. Yin, Z. Chen, R. Jenkins, C. Chen, J. Wang, W. Ma, R. Bolot, R. Lupoi, Z. Ren, H. Liao, M. Liu, Mechanical and in vitro study of an isotropic Ti6Al4V lattice structure fabricated using selective laser melting, J. Alloys Compd. 782 (2019) 209–223. https://doi.org/10.1016/j.jallcom.2018.12.220.

[48] R. Wauthle, B. Vrancken, B. Beynaerts, K. Jorissen, J. Schrooten, J.P. Kruth, J. Van Humbeeck, Effects of build orientation and heat treatment on the microstructure and mechanical properties of selective laser melted Ti6Al4V lattice structures, Addit. Manuf. 5 (2015) 77–84. https://doi.org/10.1016/j.addma.2014.12.008.

[49] S.E. Alkhatib, A. Karrech, T.B. Sercombe, Isotropic energy absorption of topology optimized lattice structure, Thin-Walled Struct. 182 (2023) 110220. https://doi.org/10.1016/j.tws.2022.110220.

[50] A. Basak, S. Das, Epitaxy and Microstructure Evolution in Metal Additive Manufacturing, Annu. Rev. Mater. Res. 46 (2016) 125–149. https://doi.org/10.1146/annurev-matsci-070115-031728.

ISSN: 2414-1895 DOI: 10.6919/ICJE.202405_10(5).0069

[51] P.C. Collins, D.A. Brice, P. Samimi, I. Ghamarian, H.L. Fraser, Microstructural Control of Additively Manufactured Metallic Materials, Annu. Rev. Mater. Res. 46 (2016) 63–91. https://doi.org/10.1146/annurev-matsci-070115-031816.

[52] X. Wu, J. Liang, J. Mei, C. Mitchell, P.S. Goodwin, W. Voice, Microstructures of laser-deposited Ti-6Al-4V, Mater. Des. 25 (2004) 137–144. https://doi.org/10.1016/j.matdes.2003.09.009.

[53] B.E. Carroll, T.A. Palmer, A.M. Beese, Anisotropic tensile behavior of Ti-6Al-4V components fabricated with directed energy deposition additive manufacturing, Acta Mater. 87 (2015) 309–320. https://doi.org/10.1016/j.actamat.2014.12.054.

[54] Y. Kok, X.P. Tan, P. Wang, M.L.S. Nai, N.H. Loh, E. Liu, S.B. Tor, Anisotropy and heterogeneity of microstructure and mechanical properties in metal additive manufacturing: A critical review, Mater. Des. 139 (2018) 565–586. https://doi.org/10.1016/j.matdes.2017.11.021.

[55] J.J. Lewandowski, M. Seifi, Metal Additive Manufacturing: A Review of Mechanical Properties, Annu. Rev. Mater. Res. 46 (2016) 151–186. https://doi.org/10.1146/annurev-matsci-070115-032024.

[56] P. Barriobero-Vila, J. Gussone, A. Stark, N. Schell, J. Haubrich, G. Requena, Peritectic titanium alloys for 3D printing, Nat. Commun. 9 (2018) 1–9. https://doi.org/10.1038/s41467-018-05819-9.

[57] D. Zhang, D. Qiu, M.A. Gibson, Y. Zheng, H.L. Fraser, D.H. Stjohn, M.A. Easton, Additive manufacturing of ultrafine-grained high-strength titanium alloys There are amendments to this paper, Nature. 576 (2019). https://doi.org/10.1038/s41586-019-1783-1.

[58] B.A. Welk, N. Taylor, Z. Kloenne, K.J. Chaput, S. Fox, H.L. Fraser, Use of Alloying to Effect an Equiaxed Microstructure in Additive Manufacturing and Subsequent Heat Treatment of High-Strength Titanium Alloys, Metall. Mater. Trans. A Phys. Metall. Mater. Sci. 52 (2021) 5367–5380. https://doi.org/10.1007/s11661-021-06475-3.

[59] Q. Chao, S. Mateti, M. Annasamy, M. Imran, J. Joseph, Q. Cai, L.H. Li, P. Cizek, P.D. Hodgson, Y. Chen, D. Fabijanic, W. Xu, Nanoparticle-mediated ultra grain refinement and reinforcement in additively manufactured titanium alloys, Addit. Manuf. 46 (2021) 102173. https://doi.org/10.1016/j.addma. 2021.10 2173.

[60] P. Huo, Z. Zhao, W. Du, Z. Zhang, P. Bai, D. Tie, Deformation strengthening mechanism of in situ TiC/TC4 alloy nanocomposites produced by selective laser melting, Compos. Part B Eng. 225 (2021) 109305. https://doi.org/10.1016/j.compositesb.2021.109305.

[61] W.H. Yu, S.L. Sing, C.K. Chua, C.N. Kuo, X.L. Tian, Particle-reinforced metal matrix nanocomposites fabricated by selective laser melting: A state of the art review, Prog. Mater. Sci. 104 (2019) 330–379. https://doi.org/10.1016/j.pmatsci.2019.04.006.

[62] M.J. Bermingham, S.D. McDonald, D.H. StJohn, M.S. Dargusch, Beryllium as a grain refiner in titanium alloys, J. Alloys Compd. 481 (2009) 20–23. https://doi.org/10.1016/j.jallcom.2009.03.016.

[63] R.W. Cahn, Binary Alloy Phase Diagrams–Second edition. T. B. Massalski, Editor-in-Chief; H. Okamoto, P. R. Subramanian, L. Kacprzak, Editors. ASM International, Materials Park, Ohio, USA. December 1990. xxii, 3589 pp., 3 vol., hard- back. \$995.00 the set, Adv. Mater. 3 (1991) 628–629.

[64] G. Choi, W.S. Choi, J. Han, P.P. Choi, Additive manufacturing of titanium-base alloys with equiaxed microstructures using powder blends, Addit. Manuf. 36 (2020) 101467. https://doi.org/10.1016/j.addma. 2020.101467.

[65] X.F. Ding, J.P. Lin, L.Q. Zhang, Y.Q. Su, G.J. Hao, G.L. Chen, A closely-complete peritectic transformation during directional solidification of a Ti-45Al-8.5Nb alloy, Intermetallics. 19 (2011) 1115–1119. https://doi.org/10.1016/j.intermet.2011.03.005.

[66] F. Appel, U. Brossmann, U. Christoph, S. Eggert, P. Janschek, U. Lorenz, J. Müllauer, M. Oehring, J.D.H. Paul, Recent progress in the development of gamma titanium aluminide alloys, Adv. Eng. Mater. 2 (2000) 699–720. https://doi.org/10.1002/1527-2648(200011)2:11<699::AID-ADEM699>3.0.CO;2-J.

[67] D.H. StJohn, The peritectic reaction, Acta Metall. Mater. 38 (1990) 631–636. https://doi.org/10.1016/0956-7151(90)90218-6.

[68] F.F. Cardoso, A. Cremasco, R.J. Contieri, E.S.N. Lopes, C.R.M. Afonso, R. Caram, Hexagonal martensite decomposition and phase precipitation in Ti-Cu alloys, Mater. Des. 32 (2011) 4608–4613. https://doi.org/10.1016/j.matdes.2011.03.040.

ISSN: 2414-1895 DOI: 10.6919/ICJE.202405_10(5).0069

[69] E. Fereiduni, A. Ghasemi, M. Elbestawi, Unique opportunities for microstructure engineering via trace B4C addition to Ti-6Al-4V through laser powder bed fusion process: As-built and heat-treated scenarios, Addit. Manuf. 50 (2022) 102557. https://doi.org/10.1016/j.addma.2021.102557.

[70] X. Wang, L.J. Zhang, J. Ning, S. Li, L.L. Zhang, J. Long, Hierarchical grain refinement during the laser additive manufacturing of Ti-6Al-4V alloys by the addition of micron-sized refractory particles, Addit. Manuf. 45 (2021) 102045. https://doi.org/10.1016/j.addma.2021.102045.

[71] X. Tian, Y. Zhu, C.V.S. Lim, J. Williams, R. Boyer, X. Wu, K. Zhang, A. Huang, Isotropic and improved tensile properties of Ti-6Al-4V achieved by in-situ rolling in direct energy deposition, Addit. Manuf. 46 (2021) 102151. https://doi.org/10.1016/j.addma.2021.102151.

[72] K. Karami, A. Blok, L. Weber, S.M. Ahmadi, R. Petrov, K. Nikolic, E. V. Borisov, S. Leeflang, C. Ayas, A.A. Zadpoor, M. Mehdipour, E. Reinton, V.A. Popovich, Continuous and pulsed selective laser melting of Ti6Al4V lattice structures: Effect of post-processing on microstructural anisotropy and fatigue behaviour, Addit. Manuf. 36 (2020) 101433. https://doi.org/10.1016/j.addma.2020.101433.

[73] G.A. Ravi, C. Qiu, M.M. Attallah, Microstructural control in a Ti-based alloy by changing laser processing mode and power during direct laser deposition, Mater. Lett. 179 (2016) 104–108. https://doi.org/10.10 16/j.matlet.2016.05.038.

[74] H. Xu, T. Tian, B. Hua, W. Zhan, L. Niu, B. Han, Q. Zhang, Effect of in-situ rolling and heat treatment on microstructure, mechanical and corrosion properties of wire-arc additively manufactured 316L stainless steel, J. Mater. Res. Technol. 27 (2023) 3349–3361. https://doi.org/10.1016/j.jmrt.2023.10.168.

[75] Y. Hu, N. Ao, S. Wu, Y. Yu, H. Zhang, W. Qian, G. Guo, M. Zhang, G. Wang, Influence of in situ micro-rolling on the improved strength and ductility of hybrid additively manufactured metals, Eng. Fract. Mech. 253 (2021). https://doi.org/10.1016/j.engfracmech.2021.107868.

[76] C.J. Todaro, M.A. Easton, D. Qiu, D. Zhang, M.J. Bermingham, E.W. Lui, M. Brandt, D.H. StJohn, M. Qian, Grain structure control during metal 3D printing by high-intensity ultrasound, Nat. Commun. 11 (2020) 1–9. https://doi.org/10.1038/s41467-019-13874-z.

[77] D. Yuan, S. Shao, C. Guo, F. Jiang, J. Wang, Grain refining of Ti-6Al-4V alloy fabricated by laser and wire additive manufacturing assisted with ultrasonic vibration, Ultrason. Sonochem. 73 (2021) 105472. https://doi.org/10.1016/j.ultsonch.2021.105472.

[78] Y. Tian, J. Shen, S. Hu, Z. Wang, J. Gou, Effects of ultrasonic vibration in the CMT process on welded joints of Al alloy, J. Mater. Process. Technol. 259 (2018) 282–291. https://doi.org/10.1016/ j.jmatprotec. 2018.05.004.

[79] W. Xu, S. Sun, J. Elambasseril, Q. Liu, M. Brandt, M. Qian, Ti-6Al-4V Additively Manufactured by Selective Laser Melting with Superior Mechanical Properties, Jom. 67 (2015) 668–673. https://doi.org/ 10.1007/s11837-015-1297-8.

[80] W. Xu, E.W. Lui, A. Pateras, M. Qian, M. Brandt, In situ tailoring microstructure in additively manufactured Ti-6Al-4V for superior mechanical performance, Acta Mater. 125 (2017) 390–400. https:// doi.org/10.1016/j.actamat.2016.12.027.

[81] Z.Z. Li, Y.Q. Yang, Z.M. Zhang, Transformation mechanism of lamellar microstructure of AZ80 wrought Mg alloy during warm deformation, Trans. Nonferrous Met. Soc. China (English Ed. 18 (2008) s156–s159. https://doi.org/10.1016/s1003-6326(10)60193-8.

[82] H. Deng, W. Qiu, S. Cao, L. Chen, Z. Hu, Y. Wei, Z. Xia, L. Zhou, X. Cui, J. Tang, Heat-treatment induced microstructural evolution and enhanced mechanical property of selective laser melted near β Ti-5Al-5Mo-5 V-3Cr-1Zr alloy, J. Alloys Compd. 858 (2021) 158351. https://doi.org/10.1016/ j.jallcom. 2020.158351.

[83] P. Lekoadi, M. Tlotleng, K. Annan, N. Maledi, B. Masina, Evaluation of heat treatment parameters on microstructure and hardness properties of high-speed selective laser melted Ti6Al4V, Metals (Basel). 11 (2021) 1–15. https://doi.org/10.3390/met11020255.

[84] N. Poondla, T.S. Srivatsan, A. Patnaik, M. Petraroli, A study of the microstructure and hardness of two titanium alloys: Commercially pure and Ti-6Al-4V, J. Alloys Compd. 486 (2009) 162–167. https://doi. org/10.1016/j.jallcom.2009.06.172.

ISSN: 2414-1895 DOI: 10.6919/ICJE.202405_10(5).0069

[85] P. Vo, E. Irissou, J.G. Legoux, S. Yue, Mechanical and microstructural characterization of cold-sprayed Ti-6Al-4V after heat treatment, J. Therm. Spray Technol. 22 (2013) 954–964. https://doi.org/10.1007/s11666-013-9945-4.

[86] G.M. Ter Haar, T.H. Becker, Laser powder bed fusion produced Ti-6Al-4V: Influence of high-energy process parameters on in-situ martensite decomposition and prior beta grain texture, J. Alloys Compd. 918 (2022) 165497. https://doi.org/10.1016/j.jallcom.2022.165497.

[87] J. Liu, K. Zhang, X. Gao, H. Wang, S. Wu, Y. Yang, Y. Zhu, A. Huang, Effects of the morphology of grain boundary α-phase on the anisotropic deformation behaviors of additive manufactured Ti–6Al–4V, Mater. Des. 223 (2022) 111150. https://doi.org/10.1016/j.matdes.2022.111150.

[88] T. Amine, J.W. Newkirk, F. Liou, Methodology for Studying Effect of Cooling Rate During Laser Deposition on Microstructure, J. Mater. Eng. Perform. 24 (2015) 3129–3136. https://doi.org/10.1007/s11665-015-1572-4.

[89] L. Xiaodan, N. Jiaqiang, Y. Jun, J. Qingyang, G. Feng, L. Weijian, Y. Guang, H. Bo, Microstructure and Anisotropy of Laser-Deposited Ti65 Titanium Alloy, Chinese J. Lasers. 50 (2023). https://www.opticsjournal.net/Articles/OJ7cb859787c698e45/Abstract.

[90] Y. Zhu, X. Tian, J. Li, H. Wang, The anisotropy of laser melting deposition additive manufacturing Ti-6.5Al-3.5Mo-1.5Zr-0.3Si titanium alloy, Mater. Des. 67 (2015) 538–542. https://doi.org/10.1016/j.matdes.2014.11.001.